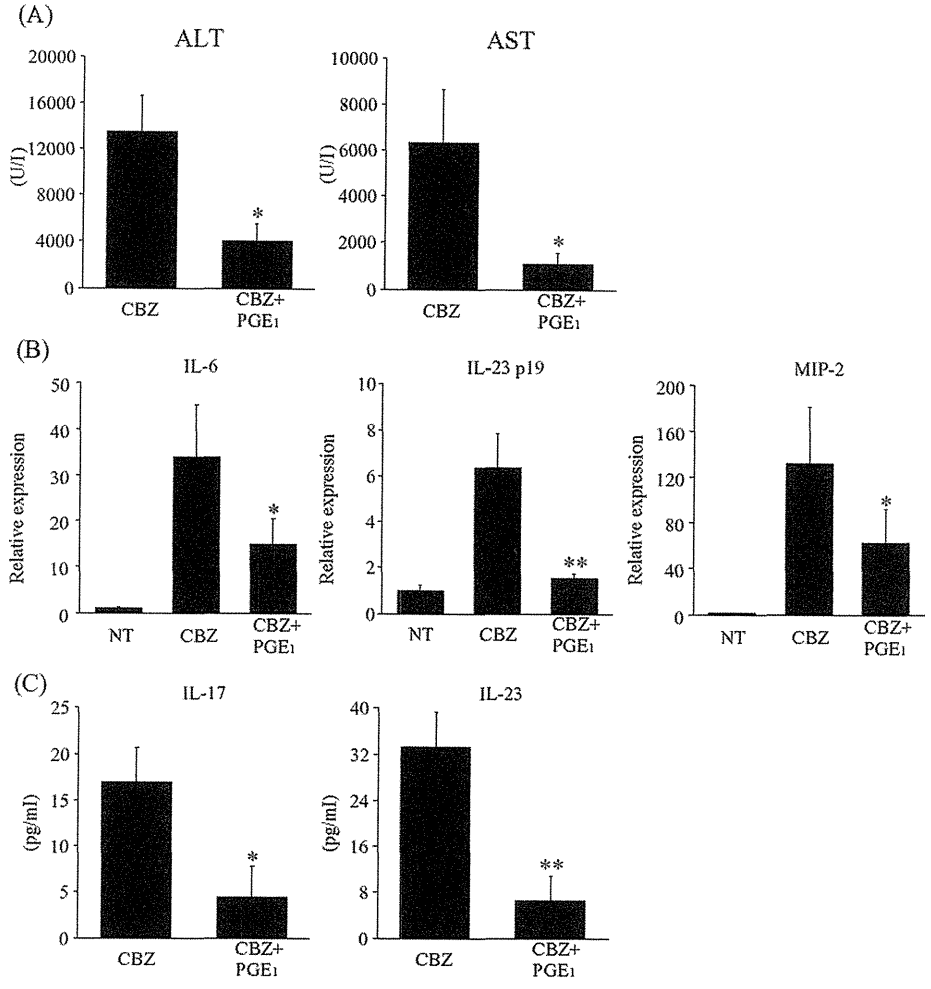


**FIG. 7.** The effects of $PGE_1$ administration on CBZ-induced liver injury. Mice were orally administered CBZ by method A, and mice were ip treated with $PGE_1$ (50 μg/mouse, dissolved in 0.5 ml sterile saline) 9 h after the last administration. As a control, vehicle was administered. At 24 h after the last CBZ administration, the livers and plasma were collected for the assessment of plasma ALT and AST levels (A), the expression levels of the hepatic mRNA of IL-6, IL-23 p19 and MIP-2 (B), and the plasma protein levels of IL-17 and IL-23 (C). The expression levels of hepatic mRNA were normalized to that of β-actin. The data are shown as the means ± SEM of the results of the method A group from seven mice and the CBZ and $PGE_1$ group from six mice. Differences compared with the CBZ-alone-administered mice were considered significant at $^*p < 0.05$ and $^{**}p < 0.01$.

1.5 h after the last administration (43.8 ± 20.7 μM) was nearly equal to the steady-state human plasma concentration of CBZ (Eichelbaum *et al.*, 1975). In clinical therapeutics, the dosage of CBZ is gradually increased for the maintenance of the therapeutic plasma concentration because CBZ is a potent inducer of microsomal drug metabolism (Oscarson *et al.*, 2006). In fact, CBZ induced the Cyp3a enzyme activity in our novel mouse model (Supplementary fig. 1). Based on our findings, it was suggested that the escalation of the dosage for the maintenance of the therapeutic plasma concentration caused the risk for CBZ-induced liver injury. In addition, the single administration of CBZ at a dose of 800 mg/kg did not induce hepatotoxicity (Fig. 2C), suggesting that repeated administration is necessary to cause CBZ-induced liver injury. Due to the presence of a specific autoantibody directed against a human liver microsomal protein in a patient who had severe hepatotoxicity with CBZ (Pirmohamed *et al.*, 1992a), the induction of drug metabolism enzymes and/or the generation of antibodies directed against CBZ-protein conjugates during repeated administration may be involved in CBZ-induced liver injury. The dosing method of CBZ in the present study might be useful for the development of animal models for other drug-induced liver injury.

In the histopathological study, remarkable hepatic necrosis and loss of hepatocytes, especially around the central vein, were observed in the mice administered CBZ by method A, and these effects were similar to APAP-induced liver injury (Antoine *et al.*, 2009). Because Cyps are mainly expressed around the central vein in the liver, this observation suggested that Cyps may be involved in CBZ-induced liver injury. CBZ-associated severe hepatotoxicity takes the following two forms: (1) a

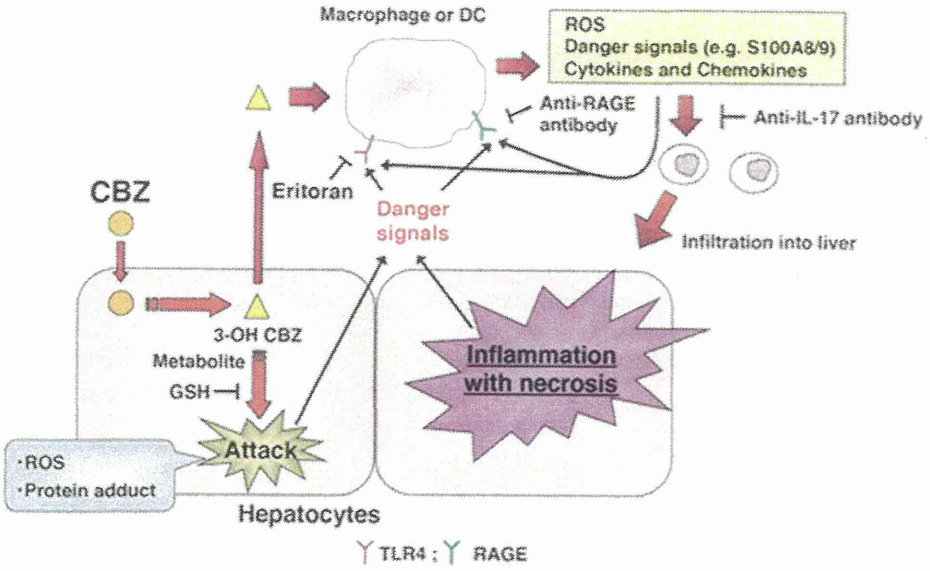


**FIG. 8.** A proposed mechanism of CBZ-induced liver injury. CBZ is metabolized in hepatocytes by Cyps, the produced reactive metabolite(s) induce ROS production in macrophages, and then danger signals released from macrophage activate TLR4 and RAGE. The activated TLR4 and RAGE lead to the secretion of proinflammatory cytokines and chemokines, which result in inflammation in the liver. The necrotic hepatocytes secrete the ligands of TLR4 and RAGE, which induce further inflammation in the liver.

hypersensitive reaction in the form of granulomatous hepatitis that present with fever and abnormal liver functions and (2) an acute hepatitis and hepatocellular necrosis with inflammation (Björnsson, 2008; Björnsson and Olsson, 2005). The mouse model in the present study may fit the latter form.

Changes in the plasma concentration of 3-OH CBZ suggested a certain role for the metabolite in CBZ-induced liver injury in the present study. Additionally, 2-OH CBZ, which is also a potential reactive metabolite, was not detected in plasma, which is coincident with a report that 2-OH CBZ is generated to a much lesser extent than 3-OH CBZ *in vitro* (Pearce *et al.*, 2002). Based on these results, 2-OH CBZ may not likely to be involved in CBZ-induced liver injury *in vivo*. It has been reported that 3-OH CBZ, a reactive metabolite produced by a variety of CYPs, induced ROS causing mitochondrial dysfunctions (Pearce *et al.*, 2008), which causes the suppression of GSH levels and the alteration of oxidative stress markers. CYP3A4 and CYP2B6 are largely responsible for the formation of 3-OH CBZ in humans (Pearce *et al.*, 2002), and these enzymes are induced by CBZ treatment. Therefore, repeated administration of a high dose of CBZ may cause the elevation of 3-OH CBZ. Because there is no direct evidence that 3-OH CBZ is a reactive metabolite or is related to the production of reactive metabolite(s), further studies are needed to examine these possibilities. In addition, 3-OH CBZ cannot be used directly for accessing hepatotoxicity due to different *in vivo* distribution and pharmacokinetics compared with CBZ. Treatment with Cyp3a inhibitors exacerbated the hepatic injury caused by CBZ (Fig. 3B), suggesting that the main function of Cyp3a is detoxification in CBZ-induced liver injury. Contrary to this result, Pirmohamed *et al.* (1992b) demonstrated that KTZ reduced the cytotoxicity of bioactivated CBZ by liver microsomes from phenobarbital-administered mice. The difference in the results between *in vitro* and *in vivo* systems is not unusual and should be carefully evaluated, especially in cases involving enzyme induction.

It has recently been reported that ROS induced the expression of the ligands of TLR4 and RAGE (Yao and Brownlee, 2010), and inflammation in the liver through the activation of TLR4 or RAGE is involved in APAP-induced liver injury (Antoine *et al.*, 2009). On the basis of these experimental results, we demonstrated that the activation of TLR4 and RAGE by ROS is the essential factor in relation to the drug metabolism and inflammation in CBZ-induced liver injury. Mu *et al.* (2011) demonstrated that the activation of TLR4 prompted the generation of Th17-associated cytokines. Therefore, the activation of TLR4 and RAGE might induce the generation of Th17-associated cytokines, resulting in inflammation in the liver in the present study.

IL-17 induced by IL-6 and IL-23 stimulates the production of CXC-chemokines (such as MIP-2 and keratinocyte-derived chemokine) and activates neutrophils (Langrish *et al.*, 2005; Steinman, 2007). IL-17 was involved in the pathogenesis of various autoimmune diseases and immune-mediated hepatotoxicity in mice (Kobayashi *et al.*, 2009, 2010). These lines of evidence prompted us to confirm the involvement of IL-17 in CBZ-induced liver injury. The neutralization of IL-17 reduced the plasma ALT and AST levels and MPO-positive cells in the liver (Figs. 6C and D), which suggested that infiltration of neutrophils into the liver via IL-17 was involved in CBZ-induced liver injury.

$PGE_1$ treatment 9 h after the last CBZ administration ameliorated CBZ-induced liver injury (Fig. 7A), and $PGE_1$ suppressed the production of IL-6 and IL-23, resulting in the decrease of plasma IL-17 concentration (Figs. 7B and C). $PGE_1$ inhibited superoxide production by neutrophils *in vitro* (Talpain *et al.*, 1995) and had a protective effect against halothane-induced liver injury by the neutralization of IL-17 in mice (Kobayashi *et al.*, 2009). Additionally, $PGE_1$ had protective effects on livers suffering from ischemia/reperfusion injury and decreased the plasma IL-6 levels in humans (Sugawara *et al.*, 1998). $PGE_1$ could be used for pharmacotherapy of CBZ-induced liver injury in clinical practice.

CBZ causes not only hepatotoxicity but also cutaneous drug reactions, including maculopapular eruption, hypersensitivity syndrome, Stevens-Johnson syndrome, and toxic epidermal necrolysis. It is well known that human leukocyte antigen alleles are strongly associated with CBZ-induced cutaneous adverse drug reactions (Hung *et al.*, 2006). In the present study, cutaneous drug reactions were not observed in the mouse model of CBZ-induced liver injury. Thus, the development of an experimental animal model of CBZ-induced cutaneous adverse drug reactions is still needed.

In conclusion, we developed a mouse model of CBZ-induced liver injury. Based on the results of the present study, the proposed mechanisms are summarized in Figure 8. Information resulting from our novel mouse model could eventually be applied to preclinical drug development.

## SUPPLEMENTARY DATA

Supplementary data are available online at http://toxsci.oxfordjournals.org/.

## FUNDING

Health and Labor Sciences Research Grants from the Ministry of Health, Labor and Welfare of Japan (H23-BIO-G001).

## REFERENCES

Ahmed, S. N., and Siddiqi, Z. A. (2006). Antiepileptic drugs and liver disease. *Seizure* **15,** 156–164.

Antoine, D. J., Williams, D. P., Kipar, A., Jenkins, R. E., Regan, S. L., Sathish, J. G., Kitteringham, N. R., and Park, B. K. (2009). High-mobility group box-1 protein and keratin-18, circulating serum proteins informative of acetaminophen-induced necrosis and apoptosis *in vivo*. *Toxicol. Sci.* **112,** 521–531.

Björnsson, E., and Olsson, R. (2005). Outcome and prognostic markers in severe drug-induced liver disease. *Hepatology* **42,** 481–489.

Björnsson, E. (2008). Hepatotoxicity associated with antiepileptic drugs. *Acta Neurol. Scand.* **118,** 281–290.

Chavakis, T., Bierhaus, A., Al-Fakhri, N., Schneider, D., Witte, S., Linn, T., Nagashima, M., Morser, J., Arnold, B., Preissner, K. T., *et al.* (2003). The pattern recognition receptor (RAGE) is a counterreceptor for leukocyte integrins: A novel pathway for inflammatory cell recruitment. *J. Exp. Med.* **198,** 1507–1515.

Eichelbaum, M., Ekbom, K., Bertilsson, L., Ringberger, V. A., and Rane, A. (1975). Plasma kinetics of carbamazepine and its epoxide metabolite in man after single and multiple doses. *Eur. J. Clin. Pharmacol.* **8,** 337–341.

Hung, S. I., Chung, W. H., Jee, S. H., Chen, W. C., Chang, Y. T., Lee, W. R., Hu, S. L., Wu, M. T., Chen, G. S., Wong, T. W., *et al.* (2006). Genetic susceptibility to carbamazepine-induced cutaneous adverse drug reactions. *Pharmacogenet. Genomics* **16,** 297–306.

Jaeschke, H., Gores, G. J., Cederbaum, A. I., Hinson, J. A., Pessayre, D., and Lemasters, J. J. (2002). Mechanisms of hepatotoxicity. *Toxicol. Sci.* **65,** 166–176.

Jin, H., Dai, J., Chen, X., Liu, J., Zhong, D., Gu, Y., and Zheng, J. (2009). Pulmonary toxicity and metabolic activation of dauricine in CD-1 mice. *J. Pharmacol. Exp. Ther.* **332,** 738–746.

Kaufman, D. W., and Shapiro, S. (2000). Epidemiological assessment of drug-induced disease. *Lancet* **356,** 1339–1343.

Kidd, P. (2003). Th1/Th2 balance: The hypothesis, its limitations, and implications for health and disease. *Altern. Med. Rev.* **8,** 223–246.

Kita, H., Mackay, I. R., Van De Water, J., and Gershwin, M. E. (2001). The lymphoid liver: Considerations on pathways to autoimmune injury. *Gastroenterology* **120,** 1485–1501.

Kobayashi, E., Kobayashi, M., Tsuneyama, K., Fukami, T., Nakajima, M., and Yokoi, T. (2009). Halothane-induced liver injury is mediated by interleukin-17 in mice. *Toxicol. Sci.* **111,** 302–310.

Kobayashi, M., Higuchi, S., Mizuno, K., Tsuneyama, K., Fukami, T., Nakajima, M., and Yokoi, T. (2010). Interleukin-17 is involved in alpha-naphthylisothiocyanate-induced liver injury in mice. *Toxicology* **275,** 50–57.

Kumada, T., Tsuneyama, K., Hatta, H., Ishizawa, S., and Takano, Y. (2004). Improved 1-h rapid immunostaining method using intermittent microwave irradiation: Practicability based on 5 years application in Toyama Medical and Pharmaceutical University Hospital. *Mod. Pathol.* **17,** 1141–1149.

Langrish, C. L., Chen, Y., Blumenschein, W. M., Mattson, J., Basham, B., Sedgwick, J. D., McClanahan, T., Kastelein, R. A., and Cua, D. J. (2005). IL-23 drives a pathogenic T cell population that induces autoimmune inflammation. *J. Exp. Med.* **201,** 233–240.

Lertratanangkoon, K., and Horning, M. G. (1982). Metabolism of carbamazepine. *Drug Metab. Dispos.* **10,** 1–10.

Lotze, M. T., Zeh, H. J., Rubartelli, A., Sparvero, L. J., Amoscato, A. A., Washburn, N. R., Devera, M. E., Liang, X., Tör, M., and Billiar, T. (2007). The grateful dead: Damage-associated molecular pattern molecules and reduction/oxidation regulate immunity. *Immunol. Rev.* **220,** 60–81.

Lu, W., and Uetrecht, J. P. (2008). Peroxidase-mediated bioactivation of hydroxylated metabolites of carbamazepine and phenytoin. *Drug Metab. Dispos.* **36,** 1624–1636.

Mu, H. H., Hasebe, A., Van Schelt, A., and Cole, B. C. (2011). Novel interactions of a microbial superantigen with TLR2 and TLR4 differentially regulate IL-17 and Th17-associated cytokines. *Cell. Microbiol.* **13,** 374–387.

Novartis Pharma Co. (2011). *Interview Form (Product Information Booklet) of Tegretol®*, 9th ed. Novartis Pharma Co.,Tokyo, Japan.

Oo, Y. H., and Adams, D. H. (2009). The role of chemokines in the recruitment of lymphocytes to the liver. *J. Autoimmun.* **34,** 45–54.

Oscarson, M., Zanger, U. M., Rifki, O. F., Klein, K., Eichelbaum, M., and Meyer, U. A. (2006). Transcriptional profiling of genes induced in the livers of patients treated with carbamazepine. *Clin. Pharmacol. Ther.* **80,** 440–456.

Park, B. K., Kitteringham, N. R., Powell, H., and Pirmohamed, M. (2000). Advances in molecular toxicology-towards understanding idiosyncratic drug toxicity. *Toxicology* **153,** 39–60.

Pearce, R. E., Lu, W., Wang, Y., Uetrecht, J. P., Correia, M. A., and Leeder, J. S. (2008). Pathways of carbamazepine bioactivation in vitro. III. The role of human cytochrome P450 enzymes in the formation of 2,3-dihydroxycarbamazepine. *Drug Metab. Dispos.* **36,** 1637–1649.

Pearce, R. E., Vakkalagadda, G. R., and Leeder, J. S. (2002). Pathways of carbamazepine bioactivation *in vitro* I. Characterization of human cytochromes

P450 responsible for the formation of 2- and 3-hydroxylated metabolites. *Drug Metab. Dispos.* **30,** 1170–1179.

Pellinen, P., Honkakoski, P., Stenbäck, F., Niemitz, M., Alhava, E., Pelkonen, O., Lang, M. A., and Pasanen, M. (1994). Cocaine N-demethylation and the metabolism-related hepatotoxicity can be prevented by cytochrome P450 3A inhibitors. *Eur. J. Pharmacol.* **270,** 35–43.

Pirmohamed, M., Kitteringham, N. R., Breckenridge, A. M., and Park, B. K. (1992a). Detection of an autoantibody directed against human liver microsomal protein in a patient with carbamazepine hypersensitivity. *Br. J. Clin. Pharmacol.* **33,** 183–186.

Pirmohamed, M., Kitteringham, N. R., Guenthner, T. M., Breckenridge, A. M., and Park, B. K. (1992b). An investigation of the formation of cytotoxic, protein-reactive and stable metabolites from carbamazepine in vitro. *Biochem. Pharmacol.* **43,** 1675–1682.

Savov, J. D., Brass, D. M., Lawson, B. L., McElvania-Tekippe, E., Walker, J. K., and Schwartz, D. A. (2005). Toll-like receptor 4 antagonist (E5564) prevents the chronic airway response to inhaled lipopolysaccharide. *Am. J. Physiol. Lung Cell Mol. Physiol.* **289,** L329–L337.

Steinman, L. (2007). A brief history of T(H)17, the first major revision in the T(H)1/T(H)2 hypothesis of T cell-mediated tissue damage. *Nat. Med.* **13,** 139–145.

Sugawara, Y., Kubota, K., Ogura, T., Esumi, H., Inoue, K., Takayama, T., and Makuuchi, M. (1998). Protective effect of prostaglandin E1 against ischemia/reperfusion-induced liver injury: Results of a prospective, randomized study in cirrhotic patients undergoing subsegmentectomy. *J. Hepatol.* **29,** 969–976.

Talpain, E., Armstrong, R. A., Coleman, R. A., and Vardey, C. J. (1995). Characterization of the PGE receptor subtype mediating inhibition of superoxide production in human neutrophils. *Br. J. Pharmacol.* **114,** 1459–1465.

Wang, H., Yang, H., and Tracey, K. J. (2004). Extracellular role of HMGB1 in inflammation and sepsis. *J. Intern. Med.* **255,** 320–331.

Yao, D., and Brownlee, M. (2010). Hyperglycemia-induced reactive oxygen species increase expression of the receptor for advanced glycation end products (RAGE) and RAGE ligands. *Diabetes* **59,** 249–255.

## SUPPLEMENTAL MATERIALS

### Detailed description of Material and Methods

#### *Determination of the plasma concentration of CBZ and its metabolites*

The plasma concentration of CBZ and its metabolites were measured using liquid chromatography tandem mass spectrometry (LC/MS/MS). Plasma (50 μL) was mixed with 500 μL dietyl ether containing 200 pmol desipramine as an internal standard. After centrifugation, the resulting supernatant was evaporated under a gentle nitrogen stream. The residue was diluted with methanol including 1% acetic acid before being subjected to LC/MS/MS. LC was performed using an HP1100 system including a binary pump, an automatic sampler, and a column oven (Agilent Technologies, Santa Clara, CA, USA), which was equipped with an Inertsil ODS-3 column (2.1 × 100 mm, 3 μm, GL Sciences, Inc.). The column temperature was 25°C. The mobile phase was 0.1% acetic acid (A) and methanol including 0.1% acetic acid (B). The conditions for elution were as follows: 10% B (0–1.0 min), 48% B (1.01–22 min), and 10% B (22.01–27 min). The flow rate was 0.2 ml/min. The LC was connected to a PE Sciex API2000 tandem mass spectrometer (Applied Biosystems) operated in the positive electrospray ionization mode. The turbo gas was maintained at 550°C. Nitrogen was used as the nebulizing, turbo, and curtain gas at 70, 40, and 50 psi, respectively. Parent and/or fragment ions were filtered in the first quadrupole and dissociated in the collision cell using nitrogen as the collision gas. CBZ and its metabolites were monitored by multiple reaction monitoring using *m/z* transitions of 237→194 (CBZ), 271→180 (trans-10,11-diOH CBZ), 253→180 (10,11-epoxide CBZ), 253→210 (2-OH CBZ), and 253→208 (3-OH CBZ). These drugs were identified by comparing the peak area to that of the authentic

standard. The analytical data were processed using Analyst software (version 1.5; Applied Biosystems, Foster City, CA, USA) in the API2000 LC-MS/MS systems.

***GSH assay***

Mouse liver was homogenized with a glass homogenizer on ice-cold 5% sulfosalicylic acid and centrifuged at 8,000 × g for 10 min. Total GSH and GSSG concentration in the supernatant were measured as described previously (Griffith, 1880). GSH was calculated from the difference between the total GSH and GSSG concentration.

***Protein carbonyl content***

Increased protein carbonyls are a stable indicator of oxidative stress. Plasma protein carbonyl content was measured using a protein carbonyl kit (Cell Biolabs, Tokyo, Japan). The assay was performed according to the manufacturer's instructions.

***Real-Time reverse transcription (RT)-PCR***

RNA from the mouse liver was isolated using RNAiso according to the manufacturer's instructions. The mRNA levels of S100A8, S100A9, HMGB1, TLR2, TLR4, TLR9, RAGE, T-bet, GATA-3, ROR-γt, IL-6, IL-12 p35, IL-23 p19, IFN-γ, FasL and MIP-2 were quantified by real-time RT-PCR. For the RT step, total RNA (10 μg) and 150 ng random hexamers were mixed and incubated at 70°C for 10 min. RNA solution was added to a reaction mixture containing 100 units of ReverTra Ace, reaction buffer and 0.5 mM dNTPs in a final volume of 40 μl. The reaction mixture was incubated at 30°C for 10 min, 42°C for 1 h, and heated at 98°C for 10 min to inactivate

the enzyme. The real-time RT-PCR was performed using the Mx3000P instrument (Stratagene, La Jolla, CA, USA). The PCR mixture contained 1 μl or 2 μl of template cDNA, SYBR Premix Ex Taq solution and 8 pmol of forward and reverse primers. Amplified products were monitored directly by measuring the increase of the dye intensity of the SYBR Green I (Molecular Probes, Eugene, OR, USA). The primer sequences are shown in Supplemental table 1.

***Measurement of plasma HMGB1, IL-17, and IL-23***

The plasma HMGB1, IL-17 and IL-23 p19 levels were measured by ELISA using the HMGB1 ELISA kit II, the Ready-SET-GO! Mouse IL-17 kit and the Ready-SET-GO! Mouse IL-23 kit according to the manufacturer's instructions, respectively.

**Supplementary methods**

Supplementary FIG. 1.

Mice were orally administered CBZ or OXC at a dose of 400 mg/kg for 4 days, and hepatic microsomes were prepared 24 h after the last administration according to the method described previously (Emoto *et al.*, 2000). Cyp3a activity was evaluated by midazolam 1'- and 4-hydroxylation using high-performance liquid chromatography according to the method of Emoto et al. (Emoto *et al.*, 2000).

**Supplementary results**

Supplementary FIG. 1.

The effects of CBZ or OXC administration on Cyp3a activity. Midazolam 1'- and 4-hydroxylase activity were significantly increased in CBZ- and OXC-administered

mice compared with NT mice. Diferences compared with the NT mice were considered significant at $**p < 0.01$.

Supplementary FIG. 2

MPO-staining in CBZ alone-administered mice or CBZ and anti-IL-17-administered mice. These samples are the same as in Figs. 6C and 6D. MPO-positive cells were significantly decreased in the mice administered CBZ and anti-IL-17 antibody compared with CBZ alone-administered mice.

**Supplemental table 1.** Sequences of primers used for real-time R TPCR analyses

| Gene | | Sequence |
|---|---|---|
| FasL | FP | AGAAGGAACTGGCAGAACTC |
| | RP | GCGGTTCCATATGTGTCTTC |
| GATA-3 | FP | GGAGGACTTCCCCAAGAGCA |
| | RP | CATGCTGGAAGGGTGGTGA |
| HMGB1 | FP | GGAGATCCTAAAAAGCCGAG |
| | RP | ATAACGAGCCTTGTCAGCCT |
| IFN-γ | FP | TCAAGTGGCATAGATGTGGAAGAA |
| | RP | TGGCTCTGCAGGATTTTCATG |
| IL-6 | FP | CCATAGCTACCTGGAGTACA |
| | RP | GGAAATTGGGGTAGGAAGGA |
| IL-12p35 | FP | TGCTGAAGACCACAGATGAC |
| | RP | GAAGTCTCTCTAGTAGCCAG |
| IL-23p19 | FP | CCAGTGTGAAGATGGTTGTG |
| | RP | CTAGTAGGGAGGTGTGAAGT |
| MIP-2 | FP | AAGTTTGCCTTGACCCTGAAG |
| | RP | ATCAGGTACGATCCAGGCTTC |
| ROR-γt | FP | ACCTCCACTGCCAGCTGTGTGCTGTC |
| | RP | TCATTTCTGCACTTCTGCATGTAGACTGTCCC |
| S100A8 | FP | GAGTGTCCTCAGTTTGTGCAG |
| | RP | TAGACATATCCAGGGACCCAG |
| S100A9 | FP | GATGGCCAACAAAGCACCTT |
| | RP | CCTCAAAGCTCAGCTGATTG |
| T-bet | FP | TGCCCGAACTACAGTCACGAAC |
| | RP | AGTGACCTCGCCTGGTGAAATG |
| TLR2 | FP | GAAAAGATGTCGTTCAAGGAG |
| | RP | TTGCTGAAGAGGACTGTTATG |
| TLR4 | FP | TTCTTCTCCTGCCTGACACC |
| | RP | CCATGCCATGCCTTGTCTTC |
| TLR9 | FP | ATTCTCTGCCGCCCAGTTTGTC |
| | RP | ACGGTTGGAGATCAAGGAGAGG |
| β-actin | FP | ACGGCCAGGTCATCACTATTGG |
| | RP | CTAGGAGCCAGAGCAGTAATCTC |

FP: Forward primer, RP: Reverse primer.

# Supplementary Fig. 1

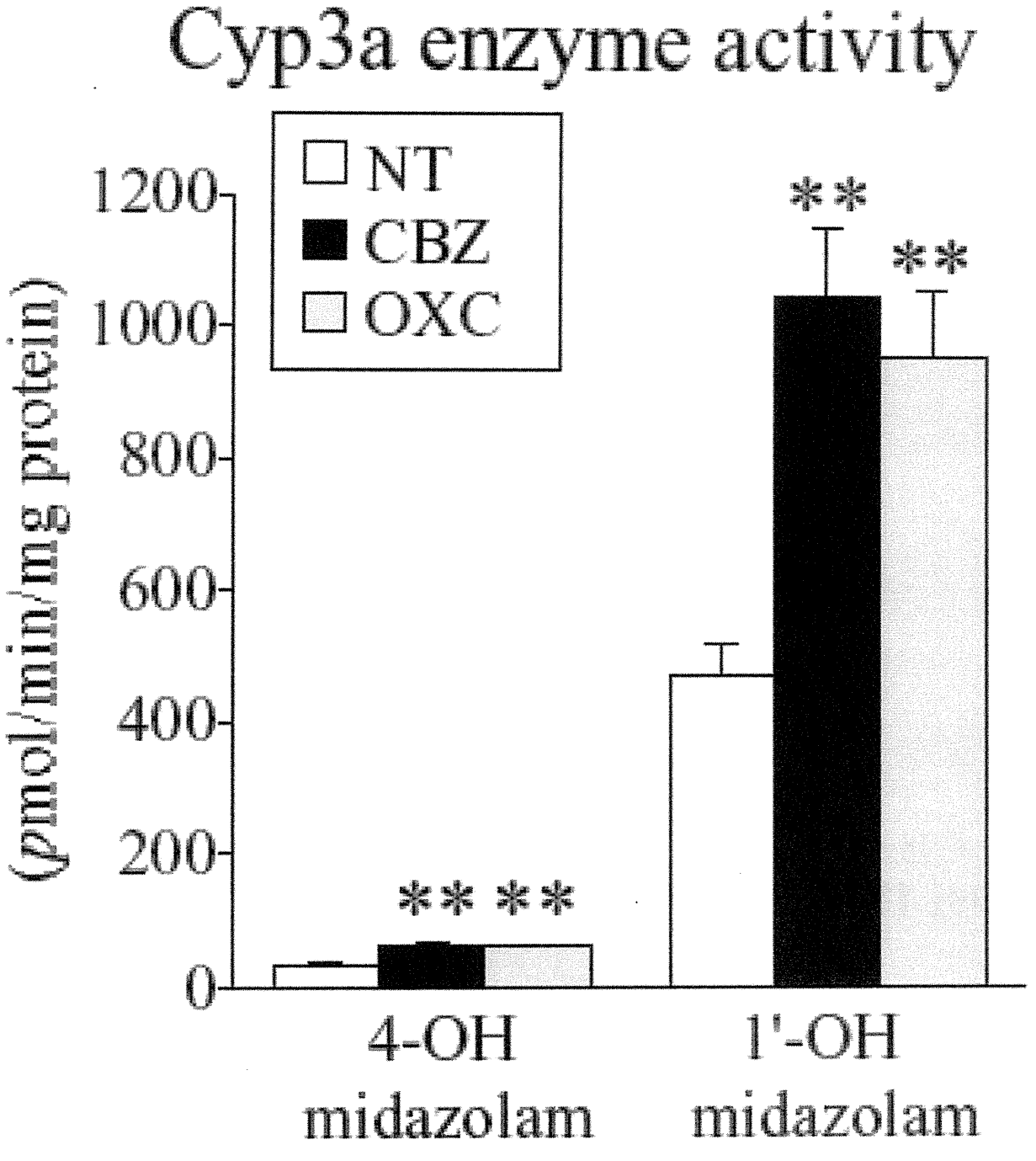

Supplementary Fig. 2

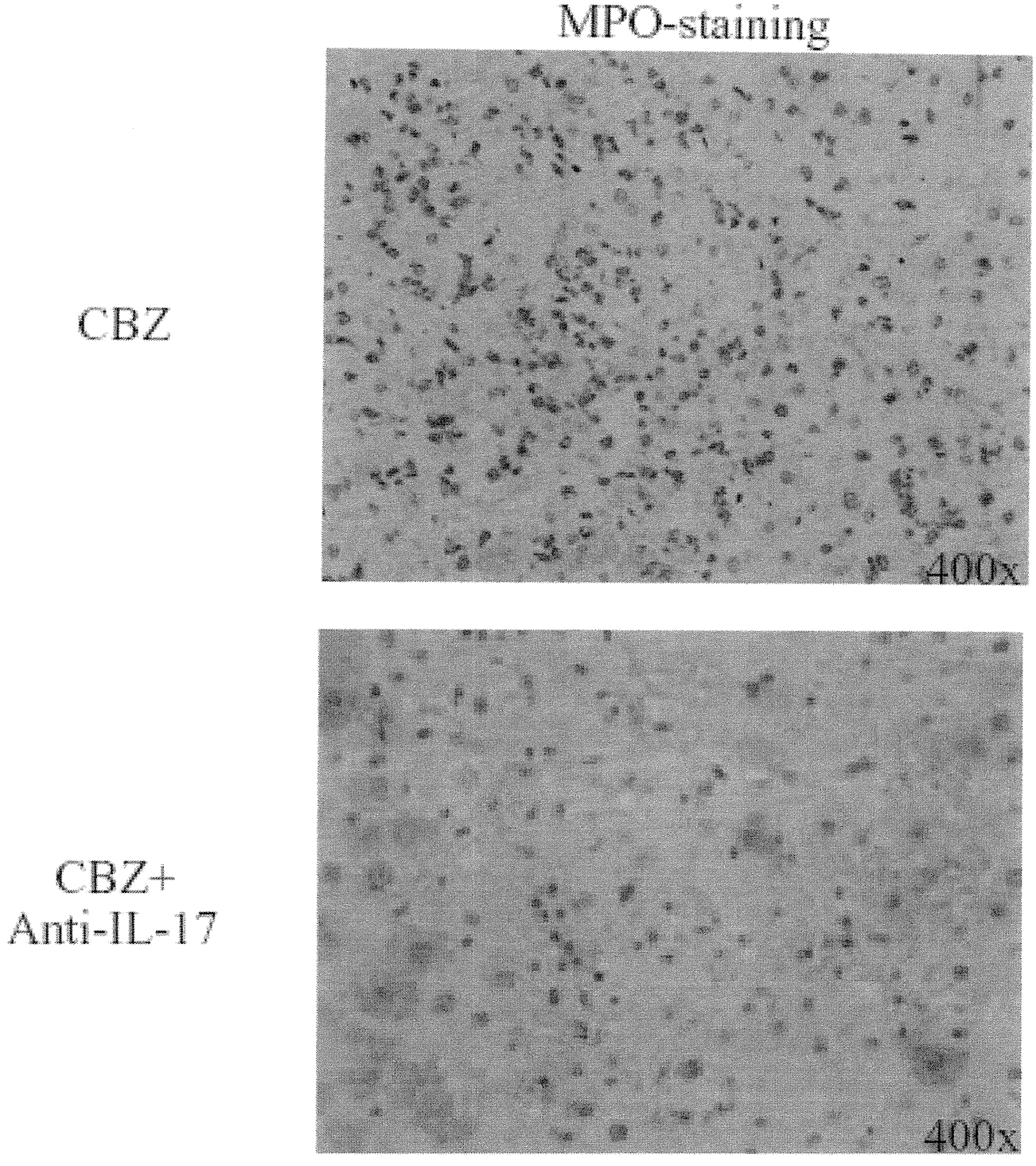

The Journal of Toxicological Sciences (J. Toxicol. Sci.)
Vol.37, No.5, 931-942, 2012



*Original Article*

# Hepatoprotective effect of tamoxifen on steatosis and non-alcoholic steatohepatitis in mouse models

**Taishi Miyashita[1], Yasuyuki Toyoda[1], Koichi Tsuneyama[2], Tatsuki Fukami[1], Miki Nakajima[1] and Tsuyoshi Yokoi[1]**

[1]*Drug Metabolism and Toxicology, Faculty of Pharmaceutical Sciences, Kanazawa University, Kakuma-machi, Kanazawa 920-1192, Japan*
[2]*Department of Diagnostic Pathology, Graduate School of Medicine and Pharmaceutical Science for Research, University of Toyama, Sugitani 930-0194, Toyama, Japan*

(Received June 9, 2012; Accepted July 3, 2012)

**ABSTRACT** — Non-alcoholic fatty liver disease (NAFLD) is characterized by hepatic lipid accumulation that starts with steatosis and progresses to non-alcoholic steatohepatitis (NASH). Recently, the number of patients with such liver diseases has increased, but the understanding of the fundamental mechanisms and appropriate therapies are lacking. Tamoxifen (TAM) is a selective estrogen receptor modulator. We previously reported that TAM plays a protective role against drug-induced and chemical-induced acute liver injuries. However, the effects of TAM on chronic liver injury, including steatosis and NASH, remain to be addressed. We first found that the administration of TAM to mouse models of steatosis and NASH significantly decreased the plasma ALT and AST levels. The administration of TAM decreased the accumulated fat and inflammation in the livers in both mouse models. In addition, we observed decreased hepatic mRNA levels of triglyceride synthesis, acyl-CoA: diacylglycerol acyltransferase 2 (DGAT2), proinflammatory cytokines, tumor necrosis factor (TNF) α, and chemokines, monocyte chemoattractant protein (MCP) -1. TAM increased the extracellular signal-regulated kinase (ERK) phosphorylation, which is related to the proliferation and regeneration of liver and to decreased DGAT2 gene expression. Furthermore, a decrease in eukaryotic translational initiation factor (eIF2α), which is involved in apoptosis, was observed in both models. These findings suggest that TAM treatment exerts a hepatoprotective effect against steatosis and NASH, presumably via up-regulation of the ERK pathways and attenuation of eIF2α activation. These pathways represent a potential therapeutic target for steatosis and NASH in drug development.

**Key words:** Steatosis, NASH, Tamoxifen, ERK

## INTRODUCTION

Non-alcoholic fatty liver disease (NAFLD) is now recognized as an important health concern (Angulo, 2002). NAFLD is characterized by hepatic lipid accumulation that starts with steatosis and progresses to non-alcoholic steatohepatitis (NASH) with progressive fibrosis. The histopathological features of NASH include evidence of steatosis, liver cell injury, a mixed inflammatory lobular infiltrate, and variable degrees of fibrosis (Ludwig *et al.*, 1980). The pathogenic mechanism of steatosis is related to fatty acid metabolism in the liver (Donnelly *et al.*, 2005). In the pathogenesis of NASH, a "two hit" theory has been proposed. Fat accumulation in the liver is the "first hit". Fat makes the liver vulnerable to endotoxins and ischemic reperfusion damage, impairs liver regeneration (Uesugi *et al.*, 2001) and causes hepatic insulin resistance (Kim *et al.*, 2001). Acyl-CoA: diacylglycerol acyltransferase 2 (DGAT2) is the final step and rate limiting reaction in triglyceride synthesis (Choi *et al.*, 2007; Yu *et al.*, 2005; Wang *et al.*, 2010). Reactive oxygen species (ROS) together with tumor necrosis factor (TNF) α and monocyte chemoattractant protein (MCP) -1 represent the "second hit" (Jou *et al.*, 2008). Fatty acids can deliver both hits. In general, chronic liver injury can be improved by diet and exercise, but fundamental medications for such liver injury have not been established.

Estrogen binds estrogen receptor and contributes to

Correspondence: Tsuyoshi Yokoi (E-mail: tyokoi@p.kanazawa-u.ac.jp)

downstream biological reactions. Estrogen receptor exists as two subtypes, estrogen receptor α and β. In the liver, estrogen receptor α is the principally expressed form, and estrogen receptor β is expressed at only low levels (Kuiper *et al.*, 1997). Estrogen-treated mice are reportedly protected from the injurious effects of hepatic ischemia and reperfusion, and estrogen protected mice from diethylnitrosamine-induced hepatocarcinogenesis (Harada *et al.*, 2004; Naugler *et al.*, 2007). These results suggest that estrogen plays a protective role in the pathology of hepatotoxicity. However, there has been little information concerning the potential functional role of estrogen after the onset of hepatotoxicity in steatosis and NASH.

Tamoxifen (TAM) is a selective estrogen receptor modulator (SERM) that can act as either an estrogen agonist or an estrogen antagonist, depending on the tissue (Dhingra, 1999). TAM acts as an antagonist in the mammary gland, but acts as an agonist in the uterus, bone tissue, and liver (Obsorne and Fuqua, 1994; Mitlak and Cohen, 1997; Cosman and Lindsay, 1999). We previously reported that TAM plays a protective role against drug-induced and chemical-induced acute liver injuries (Yoshikawa *et al.*, 2012). However, the effects of TAM on chronic liver injury, including steatosis and NASH, remain to be addressed.

In this study, we investigated whether TAM plays a protective role in mouse models of steatosis and NASH. Furthermore, we elucidated the factors that attenuate liver injury by administration of TAM.

## MATERIALS AND METHODS

### Materials

TAM was obtained from Wako Pure Chemical Industries (Osaka, Japan). Primers were commercially synthesized at Hokkaido System Sciences (Hokkaido, Japan). Monoclonal antibodies against anti-Thr202/Tyr204-phosphorylated extracellular signal-regulated kinase (ERK) 1/2, anti-Thr180/Tyr182-phosphorylated p38 mitogen-activated protein kinase (MAPK), and anti-Thr183/Tyr185 phosphorylated c-Jun N-terminal kinase (JNK) 1/2 were purchased from Cell Signaling Technology (Beverly, MA, USA). Monoclonal antibodies against ERK1/2 and JNK1/2 and the polyclonal antibodies against p38 MAPK, eukaryotic initiation factor 2 (eIF2α) and anti-Ser51-phosphorylated eIF2α were also obtained from Cell Signaling Technology. IRDye680-labeled goat anti-rabbit or anti-mouse secondary anti body and Odyssey Blocking Buffer were from Li-COR Biosciences (Lincoln, NE, USA). All other reagents were of the highest grade commercially available.

### Animal treatments

Female ICR (7 weeks old, 27-29 g) were obtained from SLC Japan (Shizuoka, Japan). Animals were housed in a controlled environment (temperature 25 ± 1°C, humidity 50 ± 10%, and 12-hr light/12-hr dark cycle) in the institutional animal facility with access to food and water *ad libitum*. Mice were fed a normal diet, high-fat-diet (HFD) or methionine and choline deficient diet (MCDD) for 10 weeks. After 9 weeks of diet, the mice were divided into 2 groups. TAM (1 mg/kg) dissolved in saline was intraperitoneally administered for 5 consecutive days. We previously reported that administration of TAM for 5 days demonstrated hepatoprotective effects against chemical-induced acute liver injuries (Yoshikawa *et al.*, 2012). Twelve hours after the final administration of TAM, the mice were sacrificed. The liver was fixed in buffered neutral 10% formalin and used for immunohistochemical staining. The degree of liver injury was assessed by hematoxylin-eosin (H&E) staining and the plasma aspartate aminotransferase (AST) and alanine aminotransferase (ALT) levels were determined using Fuji DRI-CHEM 4000V (Fuji Film Med. Co., Tokyo, Japan). Animal maintenance and treatment were conducted in accordance with the National Institutes of Health Guide for Animal Welfare of Japan, as approved by the Institutional Animal Care and Use Committee of Kanazawa University, Japan.

### GSH level

Livers (50 mg) were homogenized with ice-cold 5% sulfosalicylic acid and centrifuged at 8,000 × g at 4°C for 10 min. The GSH concentration in the supernatant was measured as described previously (Tietze, 1969).

### Lipid peroxidation measurement

Lipid peroxidation was measured using Aldetect Lipid Peroxidation Assay kit (Enzo Life Sciences, NY, USA). In brief, for each reaction, 10 μl of probucol and 640 μl of diluted R1 reagent (1:3 of methanol: N-methyl-2-phenylindole) were added to 10 mg of liver homogenate and mixed with 150 μl of 12 M HCl. Each reaction was incubated at 45°C for 60 min and centrifuged at 10,000 × g for 10 min. The supernatant was used to measure malondialdehyde (MDA) formation at 586 nm.

### Real-time reverse transcription (RT)-PCR

RNA from mouse liver was isolated using RNAiso (Takara Bio, Shiga, Japan) according to the manufacturer's instructions. Carnitine palmitoyl transferase-1 (CPT-1), acyl-CoA: diacylglycerol acyltransferase 2 (DGAT2), fatty acid synthase (FASN), monocyte chemoattractant protein (MCP) -1, sterol regulatory element-binding protein-1

(SREBP-1), tumor necrosis factor (TNF) α, and glyceraldehyde-3-phosphate dehydrogenase (Gapdh) were quantified by real-time RT-PCR. The primer sequences used in this study are shown in Table 1. The reverse transcription process, total RNA (4 μg) and 150 ng random hexamer were mixed and incubated at 70°C for 10 min. The RNA solution was added to a reaction mixture containing 100 units of ReverTra Ace, reaction buffer and 0.5 mM dNTPs in a final volume of 40 μl. The reaction mixture was incubated at 30°C for 10 min, 42°C for 1 hr and heated at 98°C for 10 min to inactivate the enzyme. The real-time RT-PCR was performed using the Mx3000P real-time PCR system (Stratagene, La Jolla, CA, USA). The PCR mixture contained 1 μl of template cDNA, SYBR Premix Ex Taq solution and 8 pmol forward and reverse primers. Amplified products were monitored directly by measurring the increase of the dye intensity of the SYBR Green I (Molecular Probes, Eugene, OR, USA) that binds to the double-strand DNA amplified by PCR.

### Immunoblot analysis

SDS-polyacrylamide gel electrophoresis and immunoblot analysis were performed. Mouse liver homogenates (50 μg) were separated on 10% polyacrylamide gels and electrotransferred onto polyvinylidene difluoride membranes, Immobilon-P (Millipore Corporation, Billerica, MA, USA). The membranes were probed with the monoclonal antibodies against anti-Thr202/Tyr204-phosphorylated ERK1/2, anti-Thr180/Tyr182-phosphorylated p38 MAPK, and anti-Thr183/Tyr185-phosphorylated JNK1/2, rabbit anti-human GAPDH antibodies, and mouse anti-KDEL antibodies and incubated with IRDye680-labeled goat anti-rabbit or anti-mouse IgG secondary antibody diluted with PBST. The Odyssey Infrared Imaging system (Li-COR Biosciences, Lincoln, NE, USA) was used for the detection. The relative expression levels were quantified using ImageQuant TL Image Analysis software (GE Healthcare, Little Chalfont, Buckinghamshire, UK).

### Statistical analysis

Data are presented as the mean ± S.D. Comparisons of 2 groups were made with an unpaired, two-tailed Student's t-test. Comparisons of multiple groups were made with ANOVA followed by Dunnett or Turkey test. A value of $P < 0.05$ was considered statistically significant.

## RESULTS

### Effects of TAM on hepatic injury in steatosis or NASH model mice

Mice were fed HFD or MCDD for 10 weeks. The plasma ALT and AST levels in steatosis and NASH mice models were significantly increased compared with CTL mice. Treatment with TAM (1 mg/kg, *i.p.*, 5 days) resulted in significantly decreased ALT and AST levels in both mouse models compared with TAM-unadministered CTL mice (Fig. 1A). Hepatocytes in the HFD-fed mice exhibited different sizes of lipid droplets and inflammation. The

**Table 1.** Sequences of primers used for real-time RT-PCR analysis in this study

| Gene | Primer | Sequence |
|---|---|---|
| CPT-1 | FP | 5'-GCA TAC CAA AGT GGA CCC CT-3' |
| | RP | 5'-TGC TCT GCA AAC ATC CAG CC-3' |
| DGAT2 | FP | 5'-CAT GAA GAC CCT CAT CGC CG-3' |
| | RP | 5'-GTG ACA GAG AAG ATG TCT TGG-3' |
| FASN | FP | 5'-GCT CCT CGC TTG TCG TCT G-3' |
| | RP | 5'-GAT CCT TCA GCT TTC CAG AC-3' |
| MCP-1 | FP | 5'-TGT CAT GCT TCT GGG CCT G-3' |
| | RP | 5'-CCT CTC TCT TGA GCT TGG TG-3' |
| SREBP-1 | FP | 5'-GAA CAG ACA CTG GCC GAG ATG-3' |
| | RP | 5'-AGG AGG CCA GAG AAG CAGAAG-3' |
| TNF-α | FP | 5'-TGT CTC AGC CTC TTC TCA TTC C-3' |
| | RP | 5'-TGA GGG TCT GGG CCA TAG AAC-3' |
| Gapdh | FP | 5'-AAA TGG GGT GAG GCC GGT-3' |
| | RP | 5'-ATT GCT GAC AAT CTT GAG TGA-3' |

FP, forward primer; RP, reverse primer.

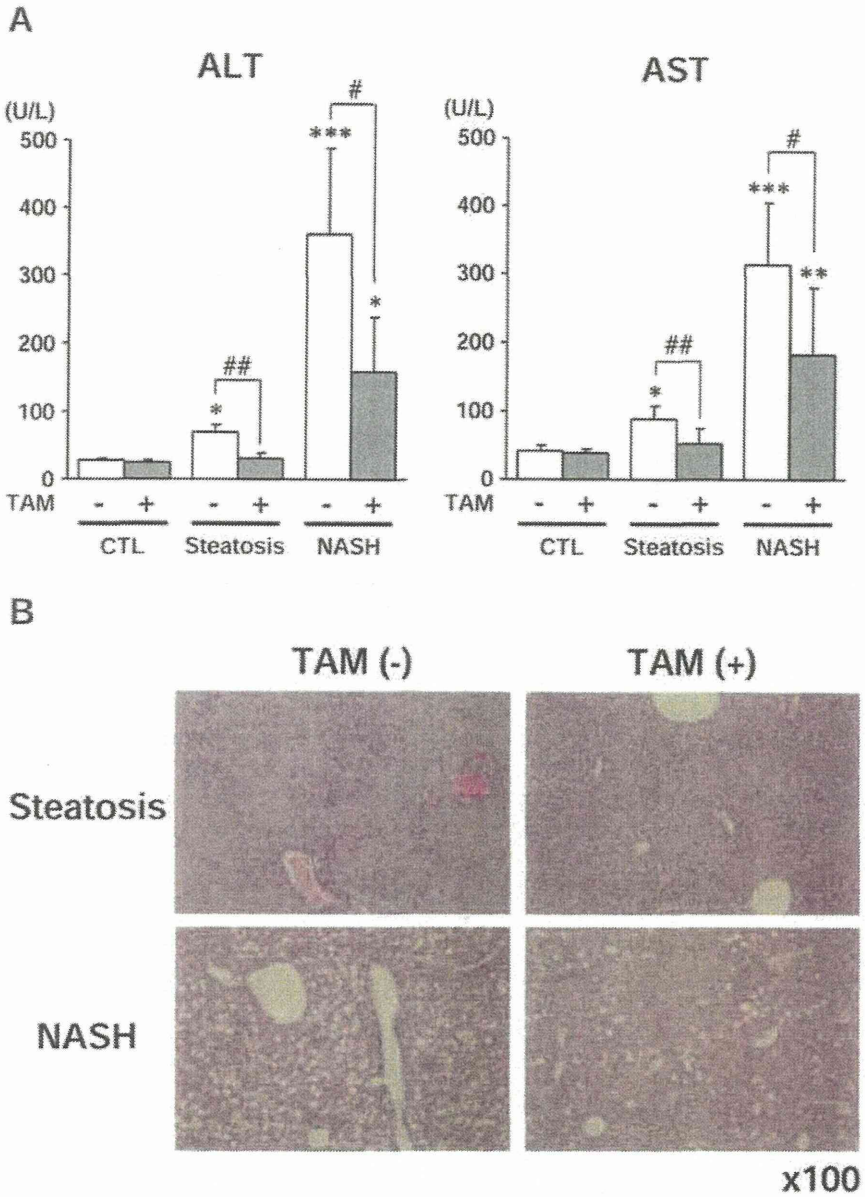


**Fig. 1.** Effects of tamoxifen (TAM) on hepatic injury in steatosis or non-alcoholic steatohepatitis (NASH) model mice. Mice were administered TAM for 5 days (1 mg/kg, *i.p.*). Plasma alanine aminotransferase (ALT) and aspartate aminotransferase (AST) levels were measured 12 hr after the last administration of TAM (A). Hematoxylin-eosin staining was performed in excised liver sections of steatosis or NASH model mice (B). Data are shown as the mean ± S.D. of results from 4-5 mice. Differences from the control (CTL) mice were considered significant at $^{*}p < 0.05$, $^{**}p < 0.01$ and $^{***}p < 0.001$, and differences from the TAM-unadministered model mice were considered significant at $^{\#}p < 0.05$ and $^{\#\#}p < 0.01$.

livers of mice fed MCDD exhibited macrovesicular steatosis, ballooning degeneration of hepatocytes, and lobular inflammation (Fig. 1B). No effect of TAM on CTL mice was observed (data not shown). Thus, feeding with HFD and MCDD for 10 weeks induced steatosis and NASH in mice. TAM-administration decreased the accumulated fat and inflammation in the livers of both mouse models. The attenuation of hepatic steatosis resulted in decreased

hepatic inflammation in TAM-administered mice.

### Effects of TAM on oxidative stress in the livers of steatosis or NASH model mice

Glutathione (GSH) detoxifies ROS produced in the mitochondrial electron transport chain (Okabe *et al.*, 1994). The ratios of GSH/ glutathione disulfide (GSSG) and MDA are often used as markers of cellular toxicity and oxidative stress and appear to increase during NAFLD progression (Caballero *et al.*, 2010). To investigate whether the oxidative stress was modulated by TAM, GSH/GSSG ratio and MDA levels in the liver were measured (Fig. 2). The ratios of GSH/GSSG in the steatosis and NASH model mice were significantly decreased compared with CTL mice, but TAM treatment produced no effect on the ratio of GSH/GSSG in the livers of the mice. MDA levels were significantly increased in steatosis and NASH model mice compared with CTL mice, but TAM had no effect on MDA (Fig. 2). These results suggest that administration of TAM is not likely to affect oxidative stress.

### Effects of TAM on hepatic mRNA expression of SREBP-1, FASN, CPT-1 and DGAT2 in steatosis or NASH model mice

The expression of genes involved in fatty acid metabolism in the liver was investigated. The expression of SREBP-1, a transcription factor that activates genes involved in lipogenesis, was unchanged in the steatosis and NASH model mice. The administration of TAM did not affect the expression of SREBP-1 in either mouse models. The expressions of FASN, an enzyme involved in fatty acid synthesis, was significantly decreased in the steatosis and NASH model mice compared with the CTL mice. In CTL mice, the expression of FASN was significantly increased by TAM, but TAM did not alter FASN expression in the steatosis and NASH model mice compared with the TAM-unadministered mice. In the steatosis model mice, the expression of CPT-1, a rate-limiting regulator of mitochondrial β-oxidation and mitochondrial fatty acid import, was significantly increased in the steatosis model mice compared with the CTL mice. The administration of TAM significantly decreased CPT-1 compared with the TAM-unadministered steatosis model mice. In the NASH model mice, the expression of CPT-1 was significantly decreased compared with the CTL mice. However, the administration of TAM did not affect the expression of CPT-1 compared with TAM-unadministered NASH model mice (Fig. 3). The expression of DGAT2, a rate limiting enzyme in triglyceride synthesis, was significantly decreased in CTL and both mouse models by TAM. These results suggest that TAM may be involved in decreasing the hepatic fat accumulation in both mouse models, and may inhibit β-oxidation of fatty acid in the steatosis model mice.

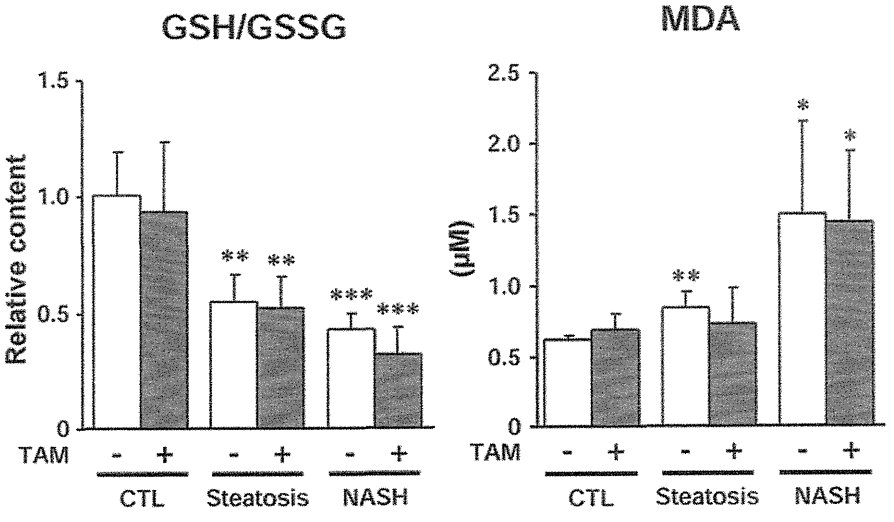


**Fig. 2.** Effects of tamoxifen (TAM) on the ratios of glutathione (GSH)/ glutathione disulfide (GSSG) and on oxidative stress in steatosis or non-alcoholic steatohepatitis (NASH) model mice. The ratios of GSH/GSSG and the malondialdehyde (MDA) levels were measured 12 hr after the last administration of TAM. Data are shown as the mean ± S.D. of results from 4-5 mice. Differences compared to the control (CTL) mice were considered significant at $*p < 0.05$, $**p < 0.01$ and $***p < 0.001$.

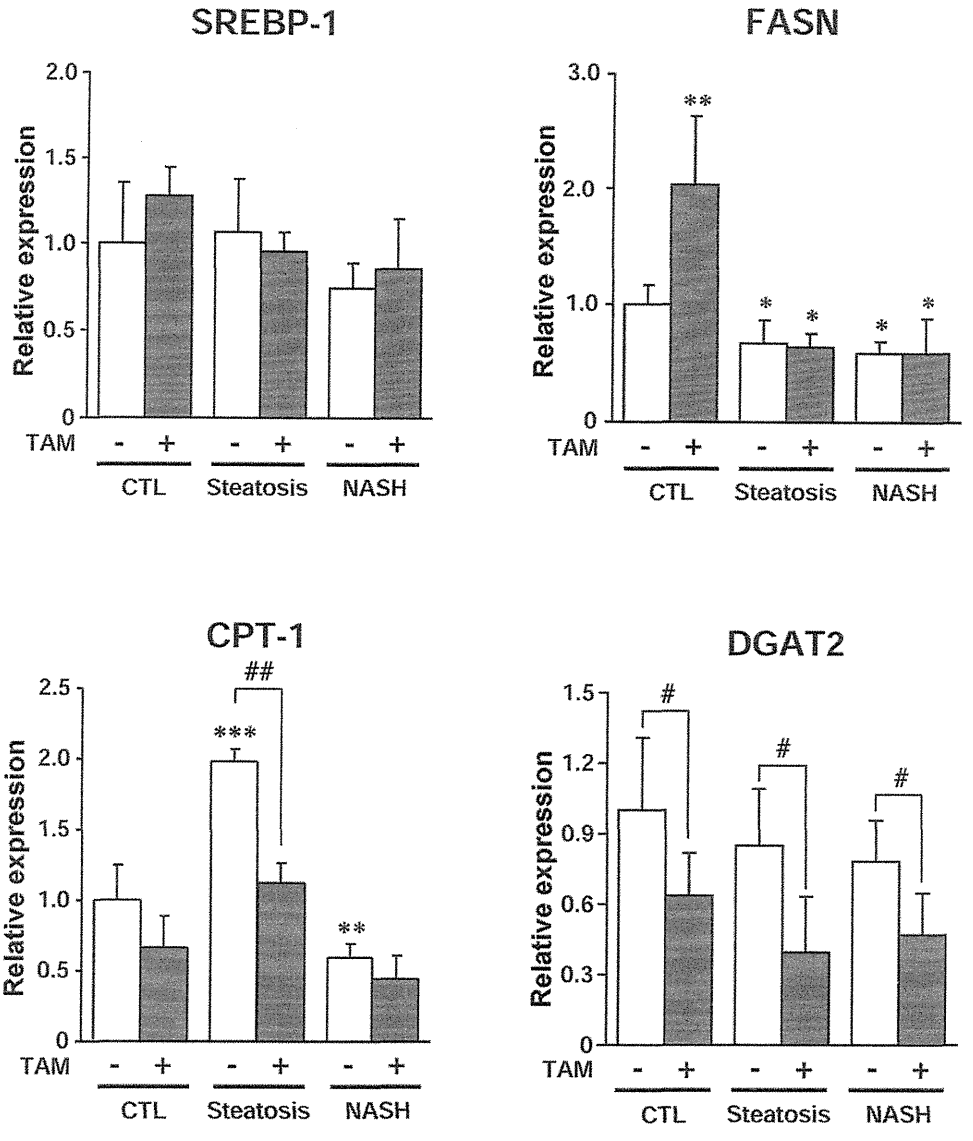


**Fig. 3.** Effects of tamoxifen (TAM) on hepatic mRNA expression of sterol regulatory element-binding protein-1 (SREBP-1), fatty acid synthase (FASN), acyl-CoA: diacylglycerol acyltransferase 2 (DGAT2) and carnitine palmonitoyl transferase-1 (CPT-1) in steatosis or non-alcoholic steatohepatitis (NASH) model mice. Mice were administered TAM for 5 days (1 mg/kg, *i.p.*). The expression of hepatic mRNA was normalized to glyceraldehyde-3-phosphate dehydrogenase (Gapdh) in each mouse. Data are shown as the mean ± S.D. of results from 4-5 mice. Differences from the control (CTL) mice were considered significant at $^{*}p < 0.05$, $^{**}p < 0.01$ and $^{***}p < 0.001$, and differences from the TAM-unadministered model mice were considered significant at $^{\#\#}p < 0.01$.

### Effects of TAM on hepatic mRNA expression of TNFα and MCP-1 in steatosis or NASH model mice

The proinflammatory cytokine TNFα and the chemokine MCP-1 are known to play an important role in the development and progression of hepatic inflammation (Anstee and Goldin, 2006). To investigate whether TAM affected the production of inflammatory cytokines and chemokines, hepatic mRNA of TNFα and MCP-1 was measured. In our previous study (Higuchi *et al.*,

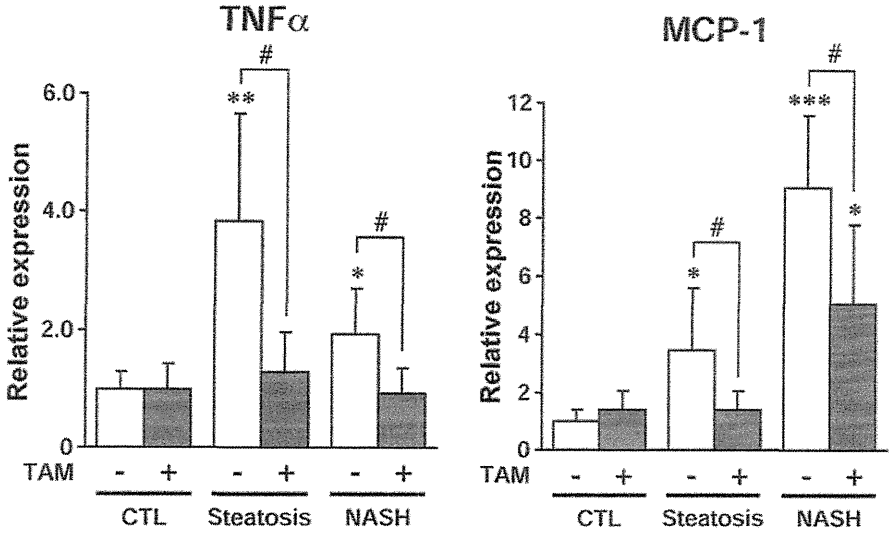


**Fig. 4.** Effects of tamoxifen (TAM) on hepatic mRNA expression of tumor necrosis factor α (TNFα) and monocyte chemoattractant protein-1 (MCP-1) in steatosis or non-alcoholic steatohepatitis (NASH) model mice. Mice were administered TAM for 5 days (1 mg/kg, *i.p.*). Expression of hepatic mRNA was normalized to glyceraldehyde-3-phosphate dehydrogenase (Gapdh) levels. Data are shown as the mean ± S.D. of results from 4-5 mice. Differences from the control (CTL) mice were considered significant at $^{*}p < 0.05$, $^{**}p < 0.01$ and $^{***}p < 0.001$, and differences from the TAM-unadministered model mice were considered significant at $^{\#}p < 0.05$.

2011), we confirmed that the expression levels of mRNA and proteins were similar for cytokines and chemokines. Thus, changes in mRNA levels were tracked in the present study. As shown in Fig. 4, the expression of TNFα and MCP-1 were significantly increased in the steatosis and NASH model mice compared with the CTL mice. Treatment with TAM significantly decreased TNFα and MCP-1 compared with TAM-unadministered mice (Fig. 5). These results suggested that the attenuation of liver injury by the administration of TAM is related to the decreased expression of inflammatory factors.

### Effects of TAM on MAPK signaling pathways in steatosis or NASH model mice

The phosphorylation of MAPK is a major component of many intracellular signaling pathways. To clarify the MAP kinase activation status, the phosphorylation of ERK1/2 (44/42 kDa), p38 MAP kinase (43 kDa), and JNK1/2 (46/54 kDa) in liver homogenates was assessed by immunoblot analysis. No significant alteration was observed in the phosphorylation of ERK in either mouse models compared to the CTL mice. Treatment with TAM resulted in a significant increase in the ERK phosphorylation in the CTL mice and both mouse models compared with the TAM-unadministered mice. However, no change was observed in the phosphorylation of p38 in either mouse models compared with the CTL mice. In addition, treatment with TAM did not affect the phosphorylation of p38. The steatosis and NASH model mice exhibited significant increases in JNK phosphorylation compared to CTL mice. Treatment with TAM produced a significant decreased in the JNK phosphorylation in the NASH model mice compared with the TAM-unadministered mice (Fig. 5). These results suggest that the attenuation of liver injury in both mouse models by treatment with TAM is related to MAPK and ERK phosphorylation in particular.

### Effects of TAM on ER stress in the liver of steatosis and NASH model mice

ER stress is caused by the accumulation of unfolded and misfolded proteins in the ER lumen and is associated with hepatic steatosis (Harding *et al.*, 2000). To investigate the mechanism of the protective effects of TAM in the mouse models, we analyzed ER stress and signaling pathways. The levels of Bip, an ER chaperone and a stress sensor protein, were increased in the liver of the steatosis and NASH model mice compared with the CTL mice. Treatment with TAM significantly decreased the

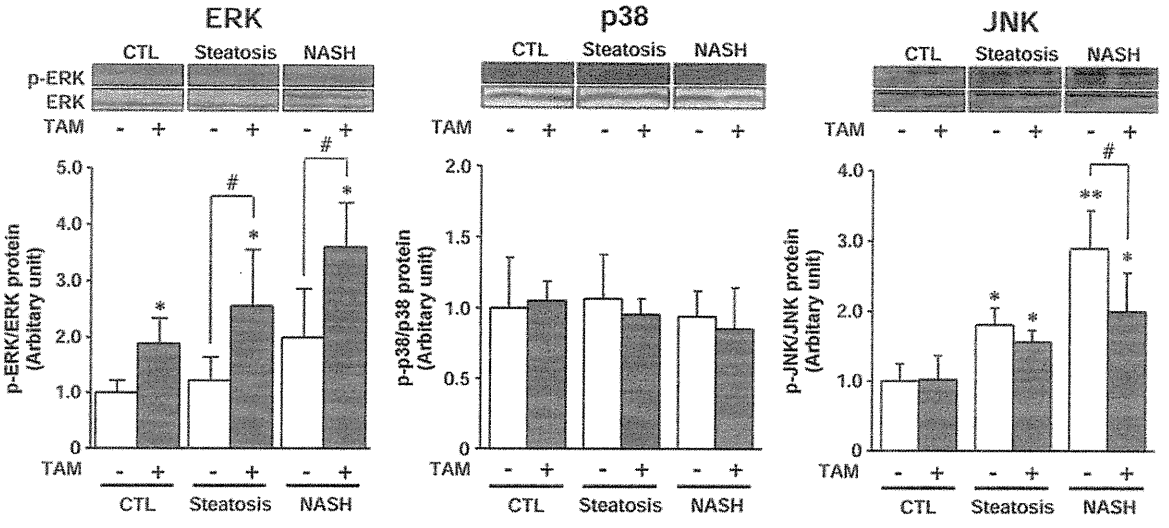


**Fig. 5.** Effects of tamoxifen (TAM) on mitogenactivated protein kinase (MAPK) signaling pathways in steatosis or non-alcoholic steatohepatitis (NASH) model mice. Mice were administered TAM for 5 days (1 mg/kg, *i.p.*). Liver homogenates (50 μg) were subjected to immunoblot analyses using antibodies to anti-Thr202/Thr204 phosphorylated extracellular signal-regulated kinase (ERK) 1/2, anti-Thr183/Thr185 phosphorylated c-Jun N-terminal kinase (JNK) 1/2 and anti-Thr180/Thr182 phosphorylated p38 MAPK. Data are shown as the mean ± S.D. of results from 4-5 mice. Differences from the control (CTL) mice were considered significant at $*p < 0.05$, $**p < 0.01$ and ***, and differences from the TAM-unadministered model mice were considered significant at $^{\#}p < 0.05$.

expression of Bip in the steatosis model mice but not in the NASH model mice compared with the TAM-unadministered mice. The levels of eIF2α, an early marker of ER stress, were increased in the NASH model mice but not in the steatosis model mice compared with the CTL mice. In addition, the levels of phosphorylated eIF2α were increased in the liver of the steatosis and NASH model mice compared with the CTL mice, whereas treatment with TAM resulted in significantly decreased eIF2α phosphorylation compared with the TAM-unadministered mice (Fig. 6). These results suggest that the attenuation of liver injury by treatment with TAM is associated with ER stress signaling.

## DISCUSSION

Steatosis and NASH are now recognized as important health concerns, and their incidences have been rising. NASH develops in patients with metabolic syndrome, and can be simulated by chronic chemical intoxication as well as by the MCDD model in experimental animals. Furthermore, it is postulated that both lipid peroxidation and ROS induce the release of TNFα and MCP-1, which may contribute to NASH (Pessayre *et al.*, 2004). In general, the HFD feeding induces hepatic steatosis without progression to steatohepatitis in rodents (Vetelainen *et al.*, 2007). Estrogen has been shown to protect against HFD-induced steatosis and is suggested to play a protective role in liver injury (Riant *et al.*, 2009; Chow *et al.*, 2011). TAM is a SERM that can act as an estrogen agonist in the liver (Obsorne and Fuqua, 1994). We previously reported that TAM has a hepatoprotective effects against various drug-induced and chemical-induced acute liver injuries (Yoshikawa *et al.*, 2012). However, there is little information about the effects of TAM on steatosis and NASH. In this study, we created steatosis and NASH model mice and investigated the effects of TAM after the onset of these liver diseases. TAM decreased the plasma ALT and AST levels in both mouse models. In addition, histopathological analysis demonstrated that TAM decreased the accumulation of fat and inflammation in the livers in both mouse models. These results indicate that TAM attenuated the liver injury in the steatosis and NASH model mice.

ROS promote oxidative damage and contribute to tissue destruction in a wide variety of diseases (Te *et al.*,

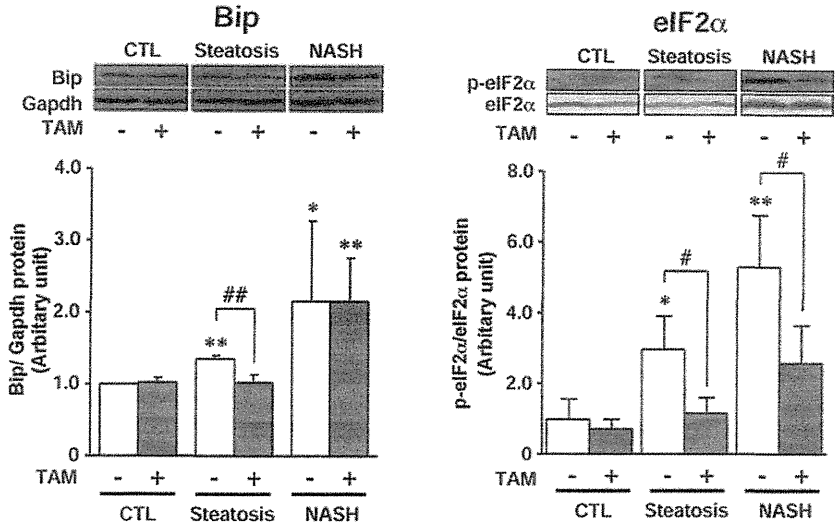


**Fig. 6.** Effects of tamoxifen (TAM) on endoplasmic reticulum (ER) stress in steatosis or non-alcoholic steatohepatitis (NASH) model mice. Mice were administered TAM for 5 days (1 mg/kg, *i.p.*). Liver homogenates (50 μg) were subjected to immunoblot analyses using antibodies to anti-KDEL, anti-Ser51 phosphorylated extracellular signal-regulated kinase (eIF2α) and anti- glyceraldehyde-3-phosphate dehydrogenase (Gapdh). Data are shown as the mean ± S.D. of results from 4-5 mice. Differences from the control (CTL) mice were considered significant at $^{*}p < 0.05$, $^{**}p < 0.01$ and ***, and differences from the TAM-unadministered model mice were considered significant at $^{\#}p < 0.05$.

2004). The ratios of GSH/GSSG and MDA levels are often used as a measurement of cellular toxicity and oxidative stress and appear to be increased in the progression of NAFLD (Caballero *et al.*, 2010; Chowdhry *et al.*, 2010). In the present study, the ratios of GSH/GSSG in the steatosis and NASH model mice were significantly decreased compared with CTL mice. In addition, MDA was significantly increased in both mouse models, but TAM had no effects on the ratio of GSH/GSSG or on MDA levels. These results indicated that TAM may not be involved in the oxidative stress, suggesting that another pathway may play a role in the attenuation of the liver injury in the steatosis and NASH model mice.

Fat accumulation in the liver can be recognized as the "first hit" in the pathogenesis of NASH. In addition, the fatty acid increase by the administration of TAM is considered one of the causes of steatosis (Cole *et al.*, 2010). In this study, the administration of TAM in the steatosis and NASH model mice did not change FASN and SREBP-1 levels, which are involved in fatty acid synthesis. However, administration of TAM decreased DGAT2 expression in CTL mice and both mouse models. DGAT2 is the rate-limiting enzyme catalyzing the final step in triglyceride synthesis and exerts an important role in the development of fatty liver diseases (Choi *et al.*, 2007; Yu *et al.*, 2005; Wang *et al.*, 2010). Thus, these results suggested that TAM did not increase but instead decreased the fat accumulation after the onset of steatosis and NASH.

Fatty acid β-oxidation occurs in both mitochondria and peroxisomes, where oxygen is available to enable the formation of ROS. In NASH, the fatty acid overload plays an important role in ROS generation as a result of electron leakage during mitochondrial β-oxidation in energy production (Haque *et al.*, 2010). Levels of CPT-1, a rate-limiting regulator of mitochondrial β-oxidation through its role in mitochondrial fatty acid import, were increased in the steatosis model mice, whereas administration of TAM significantly decreased CPT-1 levels compared to the TAM-unadministered mice. These results suggested that TAM may be related to the suppressed β-oxidation of fatty acid in the steatosis model mice.

Oxidative stress leads to inflammatory responses, including TNFα and MCP-1 (Hotamisligil, 2010). In addition, these proinflammatory cytokines and chemokines are associated with the development and progression of hepatic inflammation (Anstee and Goldin, 2006). The expressions of TNFα and MCP-1 were increased in the steatosis and NASH model mice. Treatment with TAM significantly decreased TNFα and MCP-1 in both mouse models compared with the TAM-unadministered mice